Hindawi Publishing Corporation
Advances in Acoustics and Vibration
Volume 2013, Article ID 216493, 8 pages
http://dx.doi.org/10.1155/2013/216493

Research Article

Normal Incidence of Sound Transmission Loss of a Double-Leaf Partition Inserted with a Microperforated Panel

A. Putra, A. Y. Ismail, R. Ramlan, Md. R. Ayob, and M. S. Py

Faculty of Mechanical Engineering, Universiti Teknikal Malaysia Melaka, Hang Tuah Jaya, Durian Tunggal Melaka 76100, Malaysia

Correspondence should be addressed to A. Putra; azma.putra@utem.edu.my

Received 30 April 2013; Revised 25 July 2013; Accepted 26 July 2013

Academic Editor: Rama Bhat

A double-leaf partition in engineering structures has been widely applied for its advantages, that is, in terms of its mechanical strength as well as its lightweight property. In noise control, the double-leaf also serves as an effective noise barrier. Unfortunately at low frequency, the sound transmission loss reduces significantly due to the coupling between the panels and the air between them. This paper studies the effect of a microperforated panel (MPP) inserted inside a double-leaf partition on the sound transmission loss performance of the system. The MPP insertion is proposed to provide a hygienic double-leaf noise insulator replacing the classical abrasive porous materials between the panels. It is found that the transmission loss improves at the troublesome mass-air-mass resonant frequency if the MPP is located closer to the solid panel. The mathematical model is derived for normal incidence of acoustic loading.

1. Introduction

A double-leaf structure is a common structural design for many engineering applications. The vehicle body, such as in cars, trains and airplanes, and the walls of a building are some examples of double-leaf partition in practice. From the acoustical engineering point of view, the double leaf is proposed to be a better noise barrier compared to the single-leaf. However, there remains a problem on the double-panel which is the weak sound transmission loss (STL) performance at low frequency due to the "mass-air-mass" resonance. This causes the double leaf to lose its superiority over the single-leaf [1].

Several works have been established to solve this problem. This includes employing absorptive materials inside the gap of a double-leaf, for example, fiberglass [2] and rockwool [3] which can effectively increase the STL due to additional damping to the air layer provided by the absorbent. Mao and Pietrzko [4] proposed a technique by installing the Helmholtz resonators at the air gap. The resonator acts like single degree of freedom system of which its natural frequency depends on its geometry. In order to increase the STL at mass-air-mass resonance, the Hemholtz resonator is tuned to the same resonant frequency. Li and Cheng [5] used an active control system to control the acoustic modes in the gap by using a sound source and an actuator. The sound source reduces the transmission energy by suppressing certain acoustic modes in the air gap while the actuator reduces energy from the structural path by creating counter forces on the two panels to suppress the vibration. Similarly, Li et al. [6] used long T-shaped resonators embedded along the edge of the double panel. This is also aimed to actively control both acoustics and structural path in the gap. It is found that by varying the location of the resonators, the STL at resonance can be significantly improved. Mahjoob et al. [7] introduced the newtonian fluids to control the acoustic path inside the gap. Air, oil and ferromagnetic nanoparticle fluid were used as a filler between the two panels. Although not practical, this method is also shown to increase the STL at resonance.

However, use of acoustic absorbers such as foam or fibrous type materials inside a double-panel is still the most cheapest and common practice to increase the sound insulation performance [2, 3]. For noise control application where abrasive and polluting materials cannot be presented, such as in the food industry where hygienic condition is critical to be maintained around the processing machines, conventional synthetic fibrous materials are thus not the solution. Although it is hidden between the panels, a noise barrier

panel which is easy to be cleaned handled and is free from hazardous substances to health is therefore necessary.

An alternative fiber-free absorber which has gained more popularity is a microperforated panel (MPP) absorber. MPP is a perforated panel with millimetric size holes backed by air cavity and rigid surface found by Maa in 1975. The hole diameter must be in the range between 0.05 and 1 mm and the perforation ratio between 0.5 and 1.5% for optimum absorption [8]. As the MPP can be made from panel, it provides several advantages such as nonfibrous, nonabrasive, nonpolluting, and safer in case of fire hazard. Although the MPP is mainly applied for sound absorber, several works have also been published concerning its sound insulation performance.

Dupont et al. [9] investigated the sound transmission loss of a double-leaf structure where a MPP is backed by a solid panel. Toyoda and Takahashi [10] studied the sound transmission loss of a MPP by subdividing the air cavity behind the MPP to have the sound propagation in normal incidence in the cavity. The transmission loss is found to increase at midfrequencies. Most recently, models of sound transmission loss for a multilayer partition with an MPP are proposed by Mu et al. [11]. In their model, the MPP is located at the outer layer of the system.

In this paper, a similar multilayer structure is proposed, but with the MPP inserted between two solid plates. Apart for hygienic purposes, the application can also be found in for example, a multilayer window system where a transparent panel is required to improve the noise insulation. The next section describes the derivation of the mathematical model and presents the simulation results of the effect of the MPP insertion, in terms of its location in the gap as well as its hole size and perforation ratio, on the sound transmission loss. The derivation is conducted only for the sound field with normal incidence. Recent finding suggests that the effect of mass-air-mass resonance for an infinite double-panel system subjected to the diffuse field incidence is not correct due to the internal resonance in the cavity in the direction parallel to the panel [12]. Numerical modelling technique is required, but this is beyond the scope of this paper.

2. Governing Equations

2.1. Propagating Acoustic Pressure. A mechanical system of a double-leaf inserted with an MPP (abbreviated here as DL-MPP) under normal incidence of acoustic loading can be seen in Figure 1. The solid panels are separated by distance D and the MPP is located by distance l from the back solid plate. Each of the solid and the MPP panels have mass per unit areas M and m, respectively, and they are assumed to be supported on identical mountings having stiffness per unit area s and damping constant per unit area r. The incident pressure is expressed as

$$p_i(x) = Ae^{-jkx}, \tag{1}$$

and the reflected pressure is given by

$$p_r(x) = Be^{jkx}, \tag{2}$$

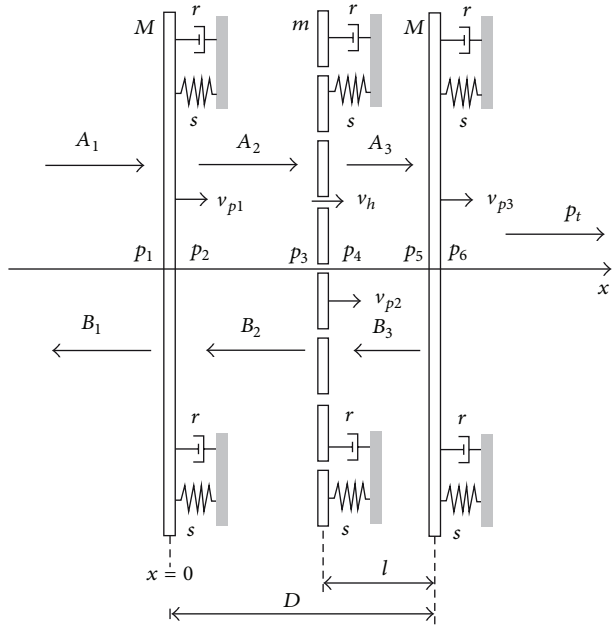

Figure 1: A schematic diagram of a DL-MPP system.

where $k = \omega/c$ for k represents the acoustic wavenumber, ω is the angular velocity, and c is the sound speed in the air. Here and for the rest of the equations, time dependence $e^{j\omega t}$ is implicitly assumed. At $x = 0$, the acoustic pressure acting on the incident side of the front panel can be written as

$$p_1 = p_i(x = 0) + p_r(x = 0) = A_1 + B_1. \tag{3}$$

In the same way as in (1) and (2), the total pressure on the other side of the front panel surface is thus

$$p_2 = A_2 + B_2. \tag{4}$$

The relation between the average surface particle velocity $\overline{v}$ and the sound pressure exciting the panel can be obtained by using Euler equation $\overline{v} = -1/j\rho\omega(dp/dx)$ [13]. For both surfaces of each panel, at $x = 0$ for the front panel this gives

$$z_f v_{p_1} = A_1 - B_1, \tag{5}$$

$$z_f v_{p_1} = A_2 - B_2, \tag{6}$$

while at $x = D - l$ for the MPP

$$\begin{aligned} z_f \overline{v} &= A_2 e^{-jk(D-l)} - B_2 e^{jk(D-l)}, \\ z_f \overline{v} &= A_3 e^{-jk(D-l)} - B_3 e^{jk(D-l)} \end{aligned} \tag{7}$$

and at $x = D$ for the back panel

$$z_f v_{p_3} = A_3 e^{-jkD} - B_2 e^{jkD}, \tag{8}$$

$$p_t = z_f v_{p_3}, \tag{9}$$

where v_p is the velocity of the panel, $\overline{v}$ is the mean particle velocity over the MPP surface, and $z_f = \rho c$ is the acoustic

impedance of air with ρ being the air density. Note that for the solid plate, the mean particle velocity on its surface equals to the velocity of the panel $\overline{v} = v_p$. This is valid for light fluid such as air and not for heavy medium such as water.

For convenience, the distance between the panel is assumed much smaller compared to the acoustic wavelength ($kD \ll 1$). The cavity pressures can therefore be assumed to be uniform between each gap

$$\begin{aligned} p_2 &\approx p_3 = A_2 + B_2 = p_b, \\ p_4 &\approx p_5 = A_3 + B_3 = p_c. \end{aligned} \tag{10}$$

Substituting (10) into (7) yields

$$z_f \overline{v} = A_2 - B_2 - jk\,(D-l)\,p_b, \tag{11}$$

$$z_f \overline{v} = A_3 - B_3 - jk\,(D-l)\,p_c. \tag{12}$$

Using the same way to the surface pressure on the back solid panel ($x = D$) gives

$$z_f v_{p_3} = A_3 - B_3 - jkDp_c. \tag{13}$$

As the cavity pressure is uniform, (5) and (11) can be combined to give

$$p_b = \frac{z_f \left(v_{p_1} - \overline{v}\right)}{jk\,(D-l)}, \tag{14}$$

while for (12) and (13), it yields

$$p_c = \frac{z_f \left(\overline{v} - v_{p_1}\right)}{jkl}. \tag{15}$$

2.2. Hole Impedance and Mean Particle Velocity. As the acoustic pressure impinges on the MPP, the air particles penetrate the holes and also excite the remaining solid surface of the panel. The combination between the panel velocity and particle velocity inside the holes creates the mean particle velocity given by [14]

$$\overline{v} = v_p\,(1-\sigma) + \sigma v_h, \tag{16}$$

where σ is the perforation ratio and v_h is the particle velocity inside the holes. The motion of fluid inside the hole depends on the impedance of the hole which according to Maa [8] is given by

$$Z_o = Z_{o,R} + Z_{o,I} \tag{17}$$

with

$$\begin{aligned} Z_{o,R} &= \frac{32 v_a t}{d_o^2}\left[\left(1 + \frac{X_o^2}{32}\right)^{1/2} + \left(\frac{\sqrt{2}X_o}{8}\right)\frac{d_o}{t}\right], \\ Z_{o,I} &= -j\rho\omega t\left[1 + \left(9 + \frac{X_o^2}{2}\right)^{-1/2} + \left(\frac{8}{3\pi}\right)\frac{d_o}{t}\right], \end{aligned} \tag{18}$$

where $X_o = (d_o/2)(\omega\rho/v_a)^{1/2}$, d_o is the hole diameter, t is the plate thickness, and v_a is the viscosity of the air, that is, 1.8×10^{-5} Ns/m^2. The real part of the impedance $Z_{o,R}$ represents the viscous effect responsible for the friction between the inner solid surface of hole and the air, and the imaginary part $Z_{o,I}$ represents the inertia of the air inside the holes of which the air moves like a piston. From these mechanisms, the net pressure Δp on the surface of the MPP can be expressed as [14]

$$Z_{o,R}\left(v_h - v_p\right) + Z_{o,I} v_h = \Delta p. \tag{19}$$

Equation (19) can also be rearranged as

$$v_h - v_p = \frac{\Delta p}{Z_o} - \frac{Z_{o,I}}{Z_o} v_p. \tag{20}$$

By substituting this into (16), the mean particle surface velocity can also be expressed as the function of the net pressure given by

$$\overline{v} = \gamma v_p + \frac{\sigma \Delta p}{Z_o}, \tag{21}$$

where $\gamma = 1 - (\sigma Z_{o,I}/Z_o)$ is the complex nondimensional terms.

2.3. Sound Transmission Loss. The equation of motion for the solid back panel is given by

$$z_{p_3} v_{p_3} = p_c - p_t, \tag{22}$$

where $z_{p_3} = z_{p_1} = j\omega M + r - js/\omega$ is the mechanical impedance of the panel. The damping constant can be written as $r = \omega_n \eta M$ with $\omega_n = (s/M)^{1/2}$ being the natural frequency of the system and η the damping loss factor. Substituting (9), (15), and (21) into (22), then dividing both sides with v_{p_3} yield the panel velocity ratio

$$\frac{v_{p_2}}{v_{p_3}} = \frac{1 + jkl\left(1 + z_{p_3}/z_f\right)}{\gamma + z_{p_2}/Z}. \tag{23}$$

The equation of motion for the MPP is expressed as

$$z_{p_2} v_{p_2} = \Delta p, \tag{24}$$

where $z_{p_2} = j\omega m + r - js/\omega$. Substituting (14), (15), and (21) into (24), and again dividing both side with v_{p_3} yield

$$\begin{aligned} \frac{v_{p_1}}{v_{p_3}} = \Bigg(\left(jk\,(D-l)\left(\frac{z_{p_2}}{z_f}\right)\right)\left[1 + jkl\left(1 + \frac{z_{p_3}}{z_f}\right)\right] \\ + \left(\gamma + \frac{z_{p_2}}{Z}\right)\left[1 + jkD\left(1 + \frac{z_{p_3}}{z_f}\right)\right]\Bigg) \\ \times \left(\gamma + \frac{z_{p_2}}{Z}\right)^{-1}. \end{aligned} \tag{25}$$

It can be seen that the velocity ratio of the solid panels depends on the location of the MPP inside the gap. From the equation of motion of the front solid panel

$$z_{p_1} v_{p_1} = p_1 - p_b \tag{26}$$

and using the relation between incident and reflected pressure in (3) and (5) it gives

$$z_{p_1} v_{p_1} = 2p_i - z_f v_{p_1} - \frac{z_f \left(v_{p_1} - \bar{v}\right)}{jk\,(D-l)}. \tag{27}$$

By dividing both sides with $p_t = z_f v_{p_3}$, the ratio of the incident and reflected pressure is given by

$$\frac{p_i}{p_t} = \frac{1}{j2k\,(D-l)} \left(\frac{v_{p_1}}{v_{p_3}} \left[1 + jk\,(D-l) \left(1 + \frac{z_{p_1}}{z_f} \right) \right] - \frac{v_{p_2}}{v_{p_3}} \left(\gamma + \frac{z_{p_2}}{Z} \right) \right). \tag{28}$$

As for plane wave, the sound power W is proportional to the sound intensity I which is simply a ratio of squared magnitude sound pressure to the air impedance, $I = |p^2|/z_f$. The transmission coefficient is therefore written as

$$\tau = \left| \frac{p_t}{p_i} \right|^2 \tag{29}$$

and the transmission loss in dB unit is

$$\mathrm{STL} = 10\log_{10} \left(\frac{1}{\tau} \right). \tag{30}$$

3. Analytical Results

3.1. Effect of MPP Location, Hole Diameter, and Perforation Ratio. Figure 2 shows the transmission loss under normal incidence of acoustic loading for double leaf (DL) [1], triple leaf (TL), and double leaf with MPP (DL-MPP) located exactly at the middle of the solid panels ($l = 0.5D$). All three panels have the same thickness of 1 mm made of aluminium (density 2700 kg/m^3) with air gap $D = 100$ mm between the solid plates. Throughout the paper, the stiffness per unit area of the mounting used in the calculation is $s = 100$ N/m^3 and the damping loss factor is $\eta = 0.01$. The graph is plotted from 50 Hz to 1 kHz to have better clarity around the resonance as well as for ease of analysis. The "mass-air-mass" resonance of the DL can be seen to occur around 170 Hz shown by the "drop" value of STL to 0 dB, a well-known phenomenon which occurs when the panels move out of phase. It can also be seen that inserting another solid panel between the double panels (TL) yields the second resonance at 280 Hz corresponding to the gap between the middle and the back panel. This can be considered to worsen the problem although the STL at mid-high frequency significantly increases due to the increase of mass. The insertion of MPP between the DLs (in the middle) overcomes the second resonance. However, the first resonance still occurs which corresponds to the gap between the solid plates.

As the aim is to improve the STL of the conventional double leaf at the resonance, Figure 3 shows the results for the DL and DL-MPP for different distance l of the MPP to the solid plate. As in Figure 2, the resonance can be seen at 170 Hz for the DL and also for the DL-MPP with MPP at

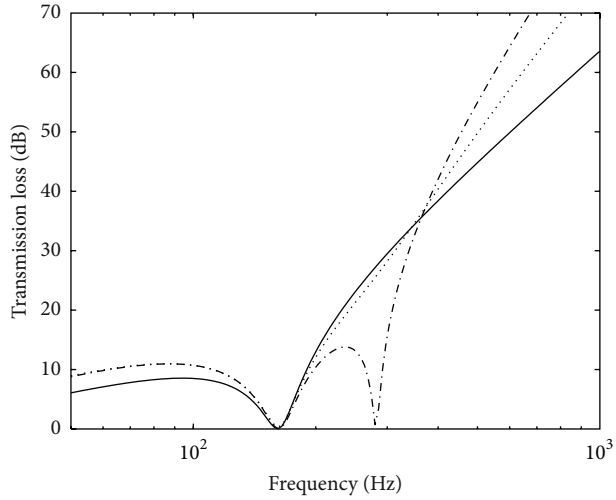

Figure 2: Comparison of sound transmission loss of — DL, – · – TL, and · · · DL-MPP (aluminium plate: $t = 1$ mm, $D = 100$ mm).

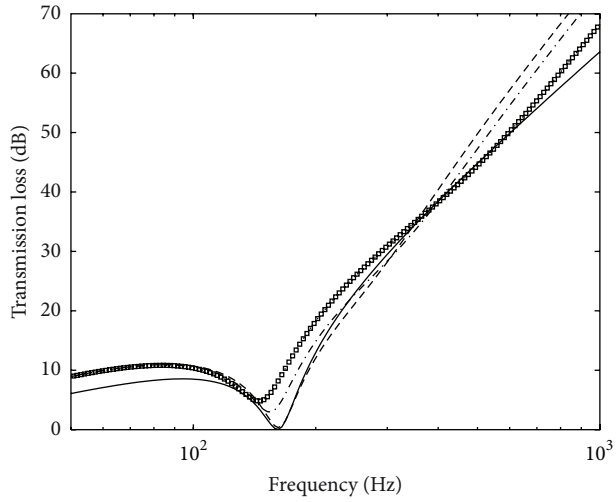

Figure 3: Comparison of sound transmission loss of DL (—) with that of DL-MPP for different locations in the gap ($d_o = 0.1$ mm, $\sigma = 1.5\%$, $D = 100$ mm; · □ · $l = 0.9D$, – – $l = 0.5D$, – · – $l = 0.2D$, and · · · $l = 0.1D$).

the middle of the gap. The presence of the MPP gives no effect to overcome the resonance in this case.

For other locations of the MPP in Figure 3, as the MPP shifts closer to the solid panel, regardless, the front or back solid panel, the STL can be observed to increase at the resonance. The additional damping due to the viscous force in the MPP holes influences the air layer in front of the solid plate which breaks the coupling between the solid panels and the air. It can also be seen that the position of the MPP in the gap also affects the STL at mid-to-high frequency in this case above 400 Hz. Contrary to the STL at resonance, the STL above the resonance increases as it moves away from the solid panel within halfway of the gap. The effect of MPP to breach the mass-air-mass resonance is also discussed by Mu et al. [11], where the MPP is located at the outer layer

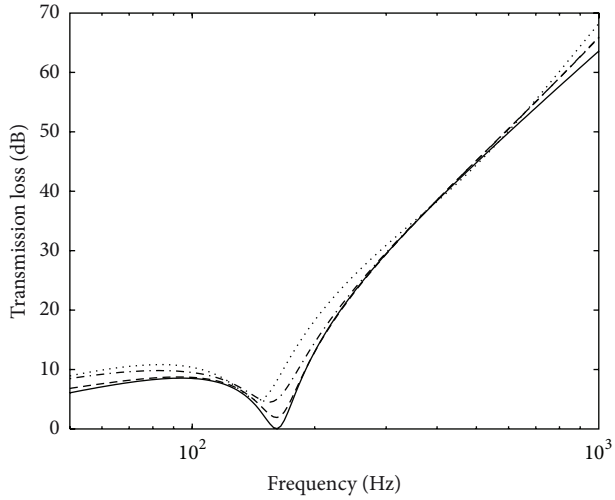

Figure 4: Comparison of sound transmission loss of DL (—) with that of DL-MPP for different hole diameters ($l = 0.1D$, $\sigma = 1.5\%$, $D = 100$ mm; $\cdots$ $d_o = 0.1$ mm, $-\cdot-$ $d_o = 0.2$ mm, and $--$ $d_o = 0.4$ mm).

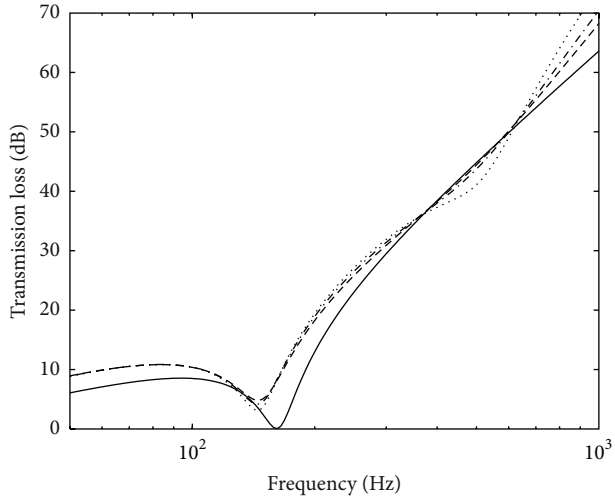

Figure 5: Comparison of sound transmission loss of DL (—) with that of DL-MPP for different perforation ratios ($l = 0.1D$, $d_o = 0.1$ mm, $D = 100$ mm; $--$ $\sigma = 0.5\%$, $-\cdot-$ $\sigma = 1.0\%$, and $\cdots$ $\sigma = 1.5\%$).

of the partition system. However, no detailed discussion is presented regarding the gap of the MPP.

Figure 4 shows the effect of hole diameter of MPP on the STL for fixed MPP location, $l = 0.1D$. Around the resonance region up to 400 Hz, decreasing the hole diameter improves the STL as this increases the domination of the real part of the hole impedance which thus provides more viscous force or damping to the MPP.

In Figure 5, the effect of the perforation ratio is investigated. It can be seen that increasing the perforation ratio does not give significant differences to the STL around the resonance. Therefore, to benefit with STL improvement at high frequency due to added mass in the system, the lowest perforation ratio for the MPP, that is, $\tau = 0.5\%$ is preferred.

Increasing the air gap of the solid plate as in Figure 6 can be seen to shift the effect of the resonance to lower frequency. The improvement at the resonance due the MPP is the same.

3.2. STL Improvement. For clarity of analysis, it is of interest to quantify the level of improvement of the STL which is the dB difference after and before inserting the MPP to the double leaf. This is also the same as the ratio of the transmitted sound power (represented by the power transmission coefficient) before (τ_b) and after (τ_a) the MPP insertion in dB unit which is given by

$$\Omega = 10\log_{10}\left(\frac{\tau_b}{\tau_a}\right) = \mathrm{STL}_a - \mathrm{STL}_b, \tag{31}$$

where STL_a is the transmission loss of the DL-MPP and STL_b is for the DL.

Figure 7 presents the STL improvement, Ω of the DL-MPP system from results in Figures 3, 4, 5, and 6 plotted up to 5 kHz to give clarity at high frequencies. In Figure 7(a), it can be seen that Ω can be achieved up to nearly 10 dB at the resonance for the MPP at $l = 0.1D$ from the solid plate.

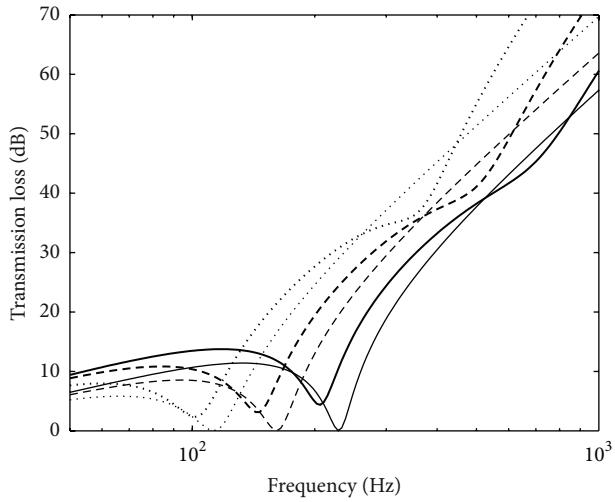

Figure 6: Comparison of sound transmission loss of DL (thick line) with that of DL-MPP (thin line) for different air gaps ($l = 0.1D$, $d_o = 0.1$ mm, $\tau = 0.5\%$; — $D = 50$ mm, $--$ $D = 100$ mm, and $\cdots$ $D = 200$ mm).

These results also show that significant improvement of 5 dB or more can be achieved for hole diameter of 2 mm or less. At higher frequency above the resonance, Ω increases rapidly with frequency by more than 20 dB/decade resembling the "mass-law" trend.

Figure 7(b) shows that smaller hole is preferred for good Ω. This could add the cost to the system as panel with smaller microholes are more difficult to fabricate. However, this can be compromised with minimum perforation ratio as shown in Figure 7(c), where almost no further improvement is given to Ω around the resonance by varying the perforation ratio. Again the effect can only be seen above the resonance at high frequency (in this case above 70 Hz), where small perforation ratio provides greater Ω.

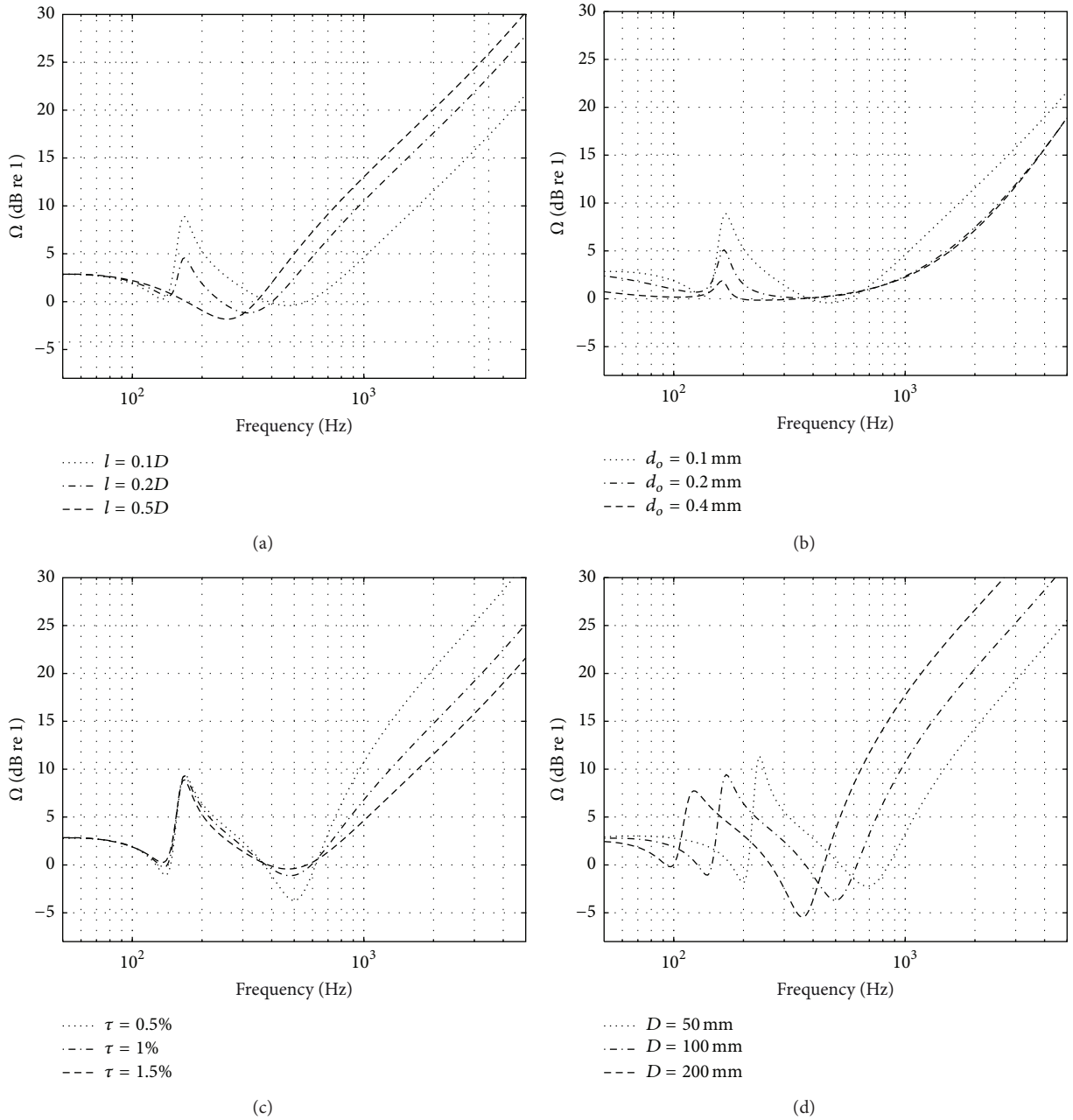

Figure 7: STL improvement of DL-MPP system with different MPP parameters: (a) locations in the gap (d_o = 1 mm, τ = 1.5%, and D = 100 mm), (b) hole diameters ($l = 0.1D$, τ = 1.5%, and D = 100 mm), (c) perforation ratio ($l = 0.1D$, d_o = 0.1 mm, and D = 100 mm), and air gap ($l = 0.1D$, d_o = 0.1 mm, and τ = 1.5%).

Figure 7(d) shows the shift of the resonance area because of the change of the air gap distance. Different peak level of Ω in the results is due to different air gap D which also results in different distance l of the MPP to the solid panel. It is also interesting to note the deterioration of Ω just after the resonance (indicated by negative Ω) which can be seen to be greater as the air gap distance is increased. As this is due to the effect of the amount of solid part in the panel, this can be reduced by increasing the perforation ratio as shown in Figure 7(c). In this case, large perforation ratio is chosen if this reduction effect cannot be tolerated in the design.

4. Experiment

The experiment to measure the transmission loss of the proposed system was conducted using the impedance tube method, where the specimen was located inside the tube and was excited by a sound field from a loudspeaker. The tube has 50 mm diameter. Two GRAS acoustic microphones 1/2 inch type 40AE were placed before the sample and the other two microphones were after the sample. The recorded signal from the microphones was then processed by a spectrum analyzer LDS Photon. The diagram of the measurement setup is shown in Figure 8.

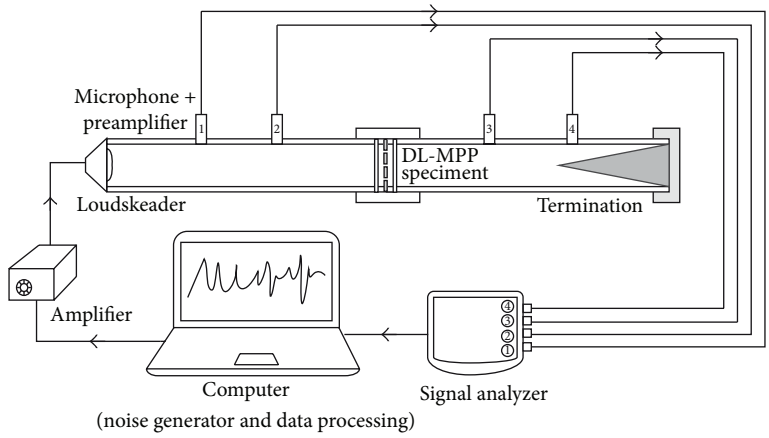

Figure 8: Diagram of the experimental setup for the sound transmission loss measurement.

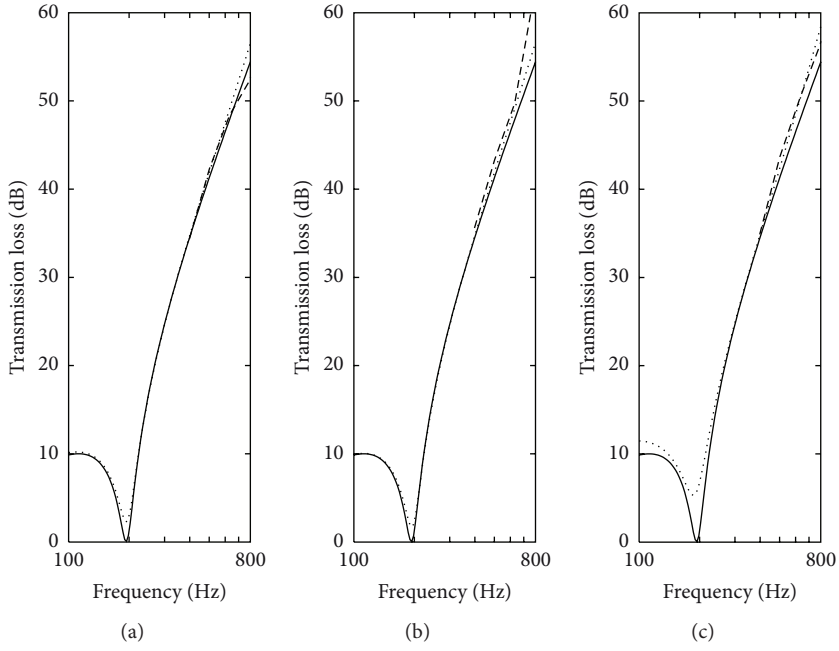

Figure 9: Transmission loss of DLMPP ($D = 70$ mm, $l = 0.15D$): (a) $d_o = 0.3$ mm, $\sigma = 0.5\%$, (b) $d_o = 0.4$ mm, $\sigma = 1\%$, and (c) $d_o = 0.5$ mm, $\sigma = 1\%$ (— theory (double panel), · · · theory (DL-MPP), and – – measured).

Three samples were prepared for the experiment, where a sample consisted of three solid 1 mm thick and round aluminium plates with diameter of also 50 mm to properly fit inside the impedance tube. The samples were fitted in a sample holder. To hold the plate sample in its position, a light tape was used between the plate perimeter and the holder. This was also to ensure that the whole plate surface can have small movement when it was exposed by a plane wave acoustic loading to closely resemble the model in Figure 1. Use of light tape was to minimise additional mass introduced to the plate. One of the plates was then perforated with submillimetric holes having diameters of 0.3 mm, 0.4 mm, and 0.5 mm for each sample. The gap between the solid plates is 70 mm and the MPP was located at 5 mm from the back solid plate.

The tube was fed with white noise up to 800 Hz to only focus the analysis at low frequency range, where the effect of mass-air-mass resonance occurs (at around 200 Hz). In this frequency range, the acoustic loading still has plane waves propagating along the tube. The signal processing technique for the transmission loss employed the wave decomposition method proposed by Salissou and Panneton [15]. This method applies two-load technique, which means that it requires two different loadings for the termination conditions for the transmission coefficient formula to be assembled. In this experiment, the loads were made from glass wool and have two different shapes: conical and circular. The former shape is to provide an anechoic termination in the tube.

Figure 9 shows the experimental results of the transmission loss for several hole diameters and perforation ratios.

The measurement data is found to be only valid from 400 Hz. This is due to the conical termination which is difficult to be anechoic at low frequencies. The reflected waves thus affect the recorded signal. This could be overcome by having a longer tube for the downstream part (i.e., the tube at the transmission region) to give the reflected waves more time to arrive at the microphone as in [11]. However, above 400 Hz, it can be seen that the measurement data shows reasonably good agreement with the theory.

5. Conclusions

The sound transmission loss of a double-leaf partition system inserted with MPP under normal incidence of acoustic loading has been reported. It is found that the MPP insertion reduces the effect of mass-air-mass resonance found in the conventional double-leaf partition at low frequency. However, this is only effective when the MPP distance is less than half of the air gap of the solid panels and improves as it approaches the solid plate. Reducing the size of the hole improves the STL at resonance, while varying the perforation ratio gives only small effect. Optimum effect of sound transmission loss improvement can therefore be achieved with small microhole diameter and small perforation ratio. At high frequency above the resonance, for any MPP parameters, the STL of the system increases dramatically due to added mass. The experimental result shows good agreement with the theory at the mass law region, but validation at low frequencies needs to be improved to observe the phenomenon at the mass-air-mass resonance. Employing the MPP for a multilayer structure is thus feasible, particularly for the system exposed with predominantly low frequency noise, for example, a window system of a control room close to a stamping machine where the sound impinges at normal direction. The proposed model can be used as a design guide.

Acknowledgment

The authors gratefully acknowledge the financial support provided for this research by the Ministry of Higher Education Malaysia (MoHE) under Fundamental Research Grant scheme no. FRGS/2010/FKM/TK02/3-F0078.

References

[1] F. J. Fahy and P. Gardonio, *Sound and Structural Vibration: Radiation, Transmission and Response*, Academic Press, London, UK, 2nd edition, 2006.

[2] W. C. Tang, H. Zheng, and C. F. Ng, "Low frequency sound transmission through close-fitting finite sandwich panels," *Applied Acoustics*, vol. 55, no. 1, pp. 13–30, 1998.

[3] J. M. Bravo, J. Sinisterra, A. Uris, J. Llinares, and H. Estelles, "Influence of air layers and damping layers between gypsum boards on sound transmission," *Applied Acoustics*, vol. 63, no. 10, pp. 1051–1059, 2002.

[4] Q. Mao and S. Pietrzko, "Control of sound transmission through double wall partitions using optimally tuned helmholtz resonators," *Acta Acustica united with Acustica*, vol. 91, no. 4, pp. 723–731, 2005.

[5] Y. Y. Li and L. Cheng, "Mechanisms of active control of sound transmission through a linked double-wall system into an acoustic cavity," *Applied Acoustics*, vol. 69, no. 7, pp. 614–623, 2008.

[6] D. Li, X.-H. Zhang, L. Cheng, and G. Yu, "Effectiveness of T-shaped acoustic resonators in low-frequency sound transmission control of a finite double-panel partition," *Journal of Sound and Vibration*, vol. 329, no. 22, pp. 4740–4755, 2010.

[7] M. J. Mahjoob, N. Mohammadi, and S. Malakooti, "An investigation into the acoustic insulation of triple-layered panels containing Newtonian fluids: theory and experiment," *Applied Acoustics*, vol. 70, no. 1, pp. 165–171, 2009.

[8] D. Y. Maa, "Theory and design of microperforated panel sound absorbing constructions," *Scientia SInica*, vol. 18, pp. 55–71, 1975 (Chinese).

[9] T. Dupont, G. Pavic, and B. Laulagnet, "Acoustic properties of lightweight micro-perforated plate systems," *Acta Acustica*, vol. 89, no. 2, pp. 201–212, 2003.

[10] M. Toyoda and D. Takahashi, "Sound transmission through a microperforated-panel structure with subdivided air cavities," *Journal of the Acoustical Society of America*, vol. 124, no. 6, pp. 3594–3603, 2009.

[11] R. L. Mu, M. Toyoda, and D. Takahashi, "Sound insulation characteristics of multi-layer structures with a microperforated panel," *Applied Acoustics*, vol. 72, no. 11, pp. 849–855, 2011.

[12] I. Prasetiyo, *Investigation of sound transmission in lightweight structures using a waveguide finite element/boundary element approach [Ph.D. thesis]*, University of Southampton, 2012.

[13] L. E. Kinsler, A. R. Frey, A. B. Coppens, and J. V. Sanders, *Fundamentals of Acoustics*, John Wiley & Sons, New York, NY, USA, 4th edition edition, 2000.

[14] D. Takahashi and M. Tanaka, "Flexural vibration of perforated plates and porous elastic materials under acoustic loading," *Journal of the Acoustical Society of America*, vol. 112, no. 4, pp. 1456–1464, 2002.

[15] Y. Salissou and R. Panneton, "A general wave decomposition formula for the measurement of normal incidence sound transmission loss in impedance tube," *Journal of the Acoustical Society of America*, vol. 125, no. 4, pp. 2083–2090, 2009.